Extended Abstracts of the 2008 International Conference on Solid State Devices and Materials, Tsukuba, 2008, pp. 176-177

H-1-3

Self-Aligned Top-Gate Nanocrystalline Silicon Thin-Film Transistors with Source/Drain Regions Activated by Diode-Pumped Continuous-Wave Green Laser

Wataru Sato[1], Akito Hara[1*], Shingo Kurauchi[1], Yoshiko Doi[1], Mitsunori Kobata[2] and Kuninori Kitahara[2]
[1]Electronic Engineering, Faculty of Engineering, Tohoku-Gakuin University, 13-1 Chuo-1, Tagajo 985-8537, Japan
[*]Corresponding author: Phone and Fax: +81-22-368-7282 E-mail: akito@tjcc.tohoku-gakuin.ac.jp
[2]Interdisciplinary Graduate School of Science and Engineering, Shimane University,1060 Nishikawatsu, Matsue 690-8504, Japan

1. Introduction

Due to their low cost and high performance, nanocrystalline (nc) silicon (Si) thin-film transistors (TFTs) are suitable for the fabrication of displays such as organic light-emitting diodes (OLEDs). Recently, a high field-effect mobility in the range of 10–150 cm^2/V s was reported in an n-channel (n-ch) nc-Si TFTs.[1–7] Furthermore, complementary metal oxide semiconductor (CMOS) inverters based on nc-Si or microcrystalline-Si TFTs have already been reported.[8]

The aim of this study is to clarify the performance of self-aligned top-gate (TG) nc-Si TFTs (L/W = 5 μm/100 μm) with laser-activated source/drain (S/D) regions. The TFTs presented here is fabricated with compatible processes with those of laser-crystallized self-aligned TG polycrystalline silicon (poly-Si) TFTs, which realize the integration of a peripheral driver circuit. We use a diode-pumped solid-state (DPSS) continuous-wave (CW) green laser (532 nm) for the laser activation. By using this laser, one of authors (A.H.) had developed high-performance TG poly-Si TFTs with average field-effect mobility of 400 cm^2/Vs, self-aligned metal double-gate poly-Si TFTs, and high-speed circuits on non-alkaline glass sustrate.[9–13] We compared the performance of laser-activated nc-Si TFTs with that of thermally activated nc-Si TFTs and found that the performance of the former is superior to that of the latter. In this study, we show that laser activation is a suitable process for the fabrication of self-aligned TG nc-Si TFTs.

2. Experiments

2-1. TFT fabrication processes

TG nc-Si TFTs with SiO_2 gate dielectric layers were fabricated on fused quartz substrates. Figure 1 shows the TFT fabrication processes. These processes were the same as those used for the fabrication of self-aligned TG poly-Si TFTs. The gate length and width were 5 μm and 100 μm, respectively. In order to investigate the crystalline properties of nc-Si in a channel region using Raman scattering, TFTs with L = 10 μm and W = 100 μm were also fabricated on identical glass substrates.

The ion implantation conditions of phosphorous were 10 KeV and 1×10^{15} cm^{-2}. The maximum process temperature of laser-activated nc-Si TFTs was 400°C, which is hydrogenation process with H_2 : Ar = 3 : 97. Thermal activation was performed at 550°C for 3 h in nitrogen gas.

2-2. Deposition of nc-Si film

The nc-Si film was directly deposited by the conventional radio frequency plasma enhanced chemical vapor deposition (rf-PECVD) method using SiH_4 diluted with H_2. The background pressure of this system was 2×10^{-5} Pa.

The optimization condition for the growth of nc-Si was determined by varying the growth conditions such as the H_2 dilution rate, temperature of the sample holding stage, rf power, and chamber pressure. We attempted to grow a Si film with a small grain size and high crystalline ratio in order to study the performance of TFTs containing the nc-Si film. For this purpose, a thin Si film having a thickness of 75 nm was deposited because the direct deposition of a thick Si film by PECVD leads to a columnar structure with a large grain size.

2-3. DPSS CW green laser for S/D activation

A DPSS CW green laser (Nd:YVO4, 2ω = 532 nm, Spectra-Physics, Millennia 8 W) was used to activate the S/D regions. The laser power was sufficiently low, and therefore, the metal (Mo) gate was not damaged and the complete melting of the Si film did not occur. The power was half of that laser power required for inducing the complete melting of the Si film.

3. Results and discussions

3-1. Growth of nc-Si thin films

Figure 2 shows the Raman scattering spectra of the Si films grown at 225°C and 325°C for 15 min at the same hydrogen dilution ratio (SiH_4 = 0.8%), an rf power of 230 mW/cm^2, and a chamber pressure of 80 Pa. In the case of the nc-Si film deposited at a low substrate temperature of 225°C, a peak corresponding to crystalline Si with a high intensity is observed at around 520 cm^{-1}. The crystallization ratios determined from the Raman spectra of the Si films grown at 225°C and 325°C were 46% and 14%, respectively.

Figure 3 shows the cross-sectional TEM image of the nc-Si film grown under the optimization conditions for 40 min. The optimized conditions are listed in Table I. From the results shown in Fig. 3, the growth speed under this condition is estimated as 1.9 nm/min.

The Raman scattering spectra of the nc-Si film, represented by the solid line in Fig. 2, was grown for 15 min under the optimized conditions listed in Table I. Thus, the film thickness (solid line in Fig. 2) was 28 nm. Although this film was very thin, we obtained a high crystallization ratio of 46%. This implied that a crystalline Si structure exists at the Si/substrate interface. This result was consistent with the results derived from the cross-sectional TEM image in Fig. 3, which shows the existence of the crystalline Si structure at the Si/substrate interface. Another important result derived from Fig. 3 is that the grain size of nc-Si is approximately 25 nm. This size was very small; thus, it was reasonable to refer to this film as a nc Si film.

3-2. TFT performance

Figure 4 shows the performance of the laser-activated TG nc-Si TFTs (L/W = 5 μm/100 μm) with a 75-nm-thick nc-Si film and a 100-nm-thick gate SiO_2 layer. An analysis shows that the field-effect mobility in the linear region is 0.5 cm^2/Vs. Figure 5 shows TFT performance of laser-activated nc-Si TFTs with gate length of 5 and 10 μm, in which gate width of both TFTs is 100 μm.

Figure 6 shows a comparison between the performance of the laser-activated TG nc-Si TFT and that of the thermally activated TG nc-Si TFT with L/W = 5 μm/100 μm. The structures of both the TFTs are identical. It is clearly observed that the performance of the laser-activated nc-Si TFT is superior to that of the thermally activated nc-Si TFT.

The difference in the performance of the two TFTs is caused due to the differences in the residual hydrogen concentration in the channel region. Micro Raman scattering measurement was performed from rear surface through glass substrate for laser-activated and thermally activated nc-Si TFTs with L/W = 10 μm/100 μm

The three-peak analysis of Si peak showed that the full width at half-maximum (FWHM) of the crystal Si peak for the laser-activated and thermally activated TFTs were 9.9 and 9.1 cm^{-1}, respectively. Furthermore, the intensity of the amorphous Si region (~480 cm^{-1}) is low for the thermally activated nc-Si TFT as compared to that for the laser-activated nc-Si TFT. This indicates that the crystallization ratio of the channel region of the thermally activated nc-Si TFT is superior to that of the laser-activated TFT, and this may be caused by solid phase crystallization during annealing of thermal activation. Despite this fact, the performance of the thermally activated nc-Si TFT is inferior to that of laser-activated nc-Si TFT.

Figure 7 shows the Raman scattering spectra for the Si-H bonding in the channel regions of the laser-activated and thermally activated nc-Si TFTs with L/W = 10 μm/100 μm. Raman scattering measurement was performed from rear surface through glass substrate. This result indicates that the residual hydrogen concentration in the channel region is higher in laser-activated TFTs than that in thermally activated TFTs. Thermal activation results in the out-diffusion of hydrogen introduced during the PECVD process. However, laser activation does not change characteristics of the nc-Si channel region because the gate metal acts as a barrier for the irradiation of laser beams, and thus, the temperature of the channel region does not increase. Thus, the laser activation is a suitable process for maintaining a high hydrogen concentration in the channel region of TG nc-Si TFTs.

The performance of the nc-Si TFTs fabricated in this experiment is inferior to that in previously reported studies. It is possible to deposit higher quality nc-Si by decreasing the substrate temperature and increasing the H_2 dilution rate. It is well known that the impurities of nc-Si influence the performance of the TFT.[3,14] Impurities such as oxygen, nitrogen, and hydrogen act as donor impurities by forming clusters.[15] A reduction in impurities will also help in improving the performance of TFTs.

4. Summary

TG nc-Si TFTs with L/W = 5 μm/100 μm were fabricated by the laser activation process using a DPSS CW green laser. It was found that the performance of laser-activated TG nc-Si TFTs was superior to that of thermally activated TG nc-Si TFTs. This indicates that laser activation is a suitable process for maintaining a high hydrogen concentration in the channel region of TG nc-Si TFTs. The activation of the S/D regions using the DPSS CW green laser may lead to the development of high performance and cost-effective system-on-glass, by using DPSS CW green laser for laser-crystallized peripheral TG poly-Si TFTs and for laser-activated pixel TG nc-Si TFTs. This is because of the low price and low maintenance cost of the DPSS CW green laser as compared to those of the excimer laser.

Acknowledgements

Part of this research was performed under the financial support from the Japan Society for the Promotion of Science (Grant-in-Aid for Scientific Research, (B) 19360165), the Foundation for Promotion of Material Science and Technology of Japan, and the Japan Science and Technology Agency (Research for Promoting Technology Seeds).

References

1) I. -C. Cheng et al.: Appl. Phys. Lett. 80 (2002) 440. 2) L. H. Teng et al.: IEEE Electron Device Lett. 24 (2003) 399. 3) C. -H. Lee et al: Appl. Phys. Lett. 86 (2005) 222106 4) S. -M. Han et al.: Tech. Dig. 2005 IEDM, p.117. 5) M. Fonrodona et al.: Thin Solid Films 501 (2006) 303. 6) C. -H. Lee et al.: IEEE Trans. Electron Devices 54 (2007) 45. 7) S. -M. Han et al.: Thin Solid Films 515 (2007) 7442. 8) C. -H. Lee et al.: 2006 MRS Symp. Proc. Vol. 910, 0910-A22-05. 9) A. Hara et al.: Tech. Dig. 2001 AM-LCD (Tokyo, 2001) p. 227. 10) A. Hara et al.: Tech. Dig. 2001 IEDM, p. 747. 11) A. Hara et al.: Jpn. J. Appl. Phys. 41 (2002) L311. 12) A. Hara et al.: Jpn. J. Appl. Phys. 43 (2004) 1269. 13) A. Hara et al.: 2003 IEDM p. 211. 14) M. Oudwan et al.: Solid-State Electronics 52 (2008) 432. 15) A. Hara: Jpn. J. Appl. Phys. 46 (2007) 46.

Table I. Optimized condition for nc-Si growth

Sub. Temp.	SiH_4	RF-power	Pressure	Growth speed
225℃	0.8%	230 mW/cm^2	80 Pa	1.9 nm/min.

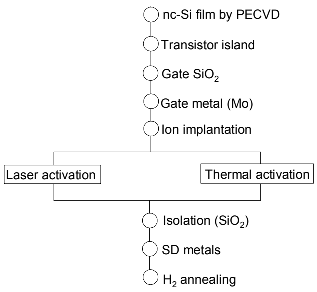

Fig. 1. TFT fabrication processes.

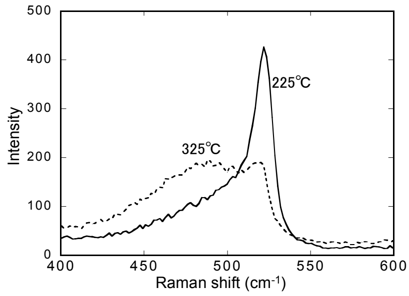

Fig. 2. Raman scattering spectra of nc-Si film grown at different substrate temperature.

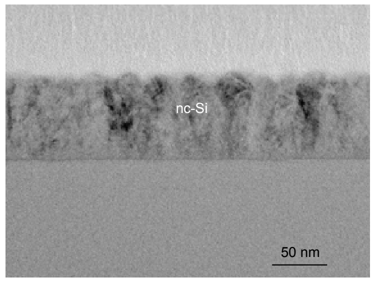

Fig. 3. Cross-sectional TEM of nc-Si grown under optimized condition for 40 minutes.

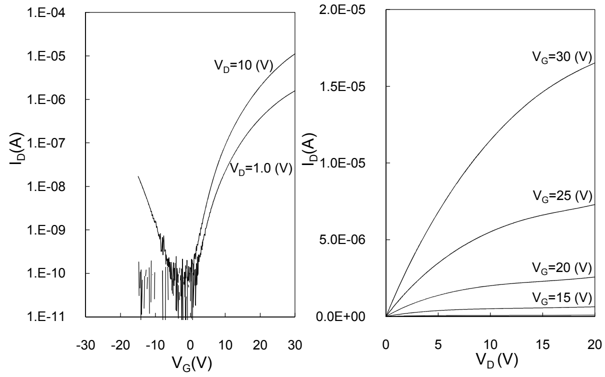

Fig. 4. TFT performance of laser-activated nc-Si TFT with L/W = 5 μm/100 μm.

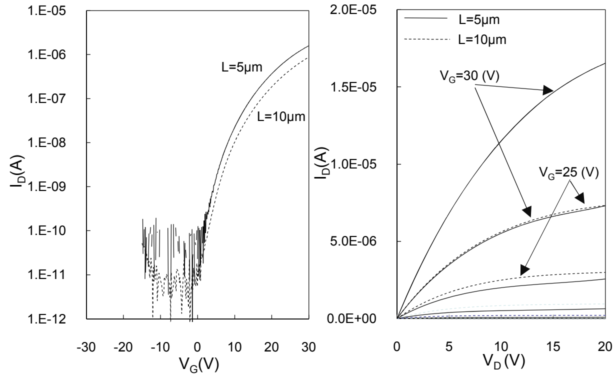

Fig. 5. TFT performance of laser-activated nc-Si TFTs with gate length of 5 μm and 10 μm.

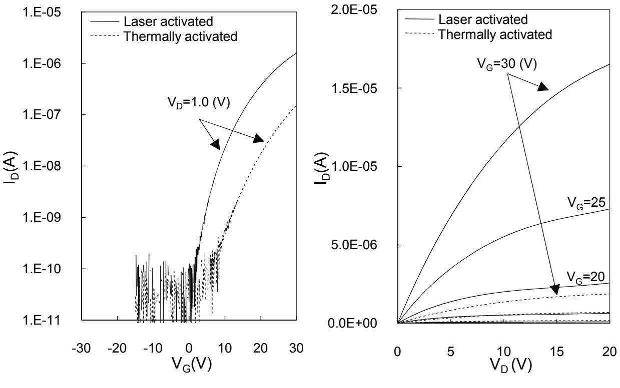

Fig. 6. Comparison of TFT performance of laser-activated and thermally activated nc-Si TFTs with L/W = 5 μm/100 μm.

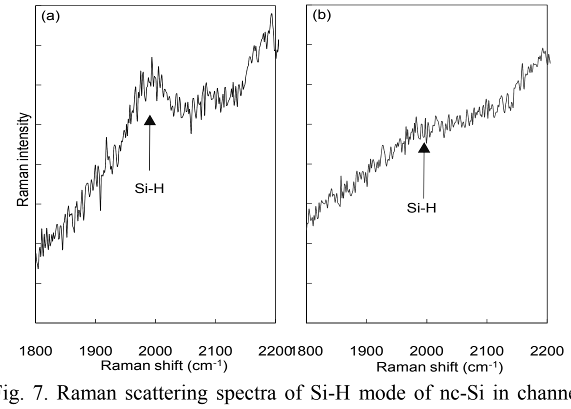

Fig. 7. Raman scattering spectra of Si-H mode of nc-Si in channel region for laser-activated (a) and thermally activated (b) nc-Si TFTs with L/W = 10 μm/100 μm.